

**Title: Chemo-ribosomal synthesis of atropisomeric and macrocyclic peptides with embedded quinolines**

**Authors:** Isaac J. Knudson, Taylor L. Dover, Diondra A. Dilworth, Cameron Paloutzian, Hannah Cho, Alanna Schepartz\*, and Scott J. Miller\*

**Abstract (158 words)**

Expanding the chemical and structural complexity of genetically encoded peptides remains a challenge in peptide therapeutics discovery. Here we report that linear peptides with a reactive  $\beta$ - or  $\gamma$ -keto amide at their *N*-termini can be synthesized ribosomally using in vitro translation methods. We show that peptides carrying an *N*-terminal  $\beta$ -keto amide can be converted into diverse heterocyclic quinoline-peptide hybrids via Friedländer reactions with a variety of 2-aminoarylcarbonyl co-substrates. Reactions with appropriately substituted 2-aminobenzophenones generated quinoline-peptide hybrids with stable biaryl atropisomeric axes. In vitro-translated peptides carrying both an *N*-terminal  $\beta$ -keto amide and an internal 2-aminoacetophenone motif undergo intramolecular Friedländer macrocyclization reactions that embed a quinoline pharmacophore directly within the macrocyclic backbone. The introduction of *N*-terminal ketide building blocks into genetically encoded materials and their post-translational derivatization with carbonyl chemistry simultaneously expands the chemical diversity and structural complexity of genetically encoded materials and provides a paradigm for the programmed synthesis of peptide-derived materials that more closely resemble complex natural products.

## Introduction

From the first clinical application of insulin in 1921<sup>1,2</sup> to the recent triumph of GLP-1 agonists<sup>3,4</sup>, peptides have proven a valuable therapeutic modality. Advances in genetic code reprogramming, biological display, and computational design have set the stage for the next generation of peptide-derived therapeutics<sup>5</sup>. The first wave of these compounds represent some of the most exciting therapeutic candidates of the past decade because of their antibody-like affinity for traditionally “undruggable” targets such as protein-protein interfaces, while also showing promise for oral or intracellular delivery. Several therapeutic candidates derived from *de novo* peptide leads have progressed into clinical trials or onto the market<sup>6–13</sup>. In each of these cases, the initial lead identified by mRNA or phage display required extensive modification to improve its physicochemical properties<sup>10</sup>. Modifications introduced during lead optimization often include the installation of one or more macrocyclic rings and other backbone alterations that enhance protease resistance, target affinity, bioavailability, and/or cell permeability<sup>14,15</sup>. Chemical strategies to install these modifications earlier in the drug discovery process—ideally, prior to biological display—would offer distinct advantages.

Many strategies exist to install macrocyclic rings within peptides before or after biological display. Common methods include disulfide formation between Cys side chains, thioether formation between a Cys side chain and a terminal chloroacetamide or benzyl halide, copper-catalyzed azide-alkyne cycloaddition, amide bond-forming reactions<sup>16–18</sup>, and a variety of metal-catalyzed macrocyclizations<sup>19–21</sup>. Although widely employed, each of these methods suffers from at least one liability with respect to downstream applications and none provide added value: Disulfide bonds are reversible, while thioethers are flexible and, like click reaction products, prone to oxidation. Alternative macrocyclization strategies that generate stable and drug-like linkers are widely recognized as an unmet need<sup>9,22–27</sup>. Chemistry that exploits the macrocyclization event to establish a known pharmacophore within the peptide backbone prior to biological display is a promising strategy towards this end<sup>28</sup>.

Quinolines are an established class of aromatic pharmacophores replete in natural products, FDA-approved drugs, and high-affinity ligands for both protein and RNA. Quinoline-containing small molecules that engage proteins include FDA-approved therapeutics such as chloroquine, moxifloxacin, topotecan, lenvatinib, and saquinavir, which is itself a peptidomimetic with an *N*-terminal quinoline<sup>29,30</sup>. Quinolines are especially privileged with respect to RNA<sup>31–34</sup>. Quinoline-peptide conjugates function as helix-threading intercalators<sup>35,36</sup>, and substituted quinolines are found within small molecules that target pre-mRNA to modulate splicing<sup>37</sup>. Perhaps the most unique aspect of the quinoline pharmacophore is its ability to support axial chirality and exist, in certain cases, as stable atropisomers. This stereochemical complexity would add a new level of topological diversity to genetically encoded linear or cyclic peptides.

Recently, we reported that linear peptides with a  $\beta$ -dicarbonyl functionality at the *N*-terminus could be synthesized ribosomally using *in vitro* translation to generate novel  $\beta$ -dicarbonyl-peptide hybrid molecules<sup>38</sup>. Other  $\beta$ -dicarbonyl functionality could be introduced into polypeptides using orthogonal aminoacyl-tRNA synthetases<sup>39</sup>. In both cases, the

$\beta$ -dicarbonyl species reported were derivatives of malonic acid, which are among the least reactive of all 1,3-dicarbonyl species, especially under mild conditions. We hypothesized that if we could ribosomally incorporate a more reactive  $\beta$ -dicarbonyl species at the *N*-terminus, then the resulting peptide or protein could be modified post-translationally into a heterocyclic pharmacophore using any one of a number of classic or modern chemical transformations. If the post-translational modification made use of a side chain as a co-substrate, then the resulting macrocycle would contain an embedded heterocycle. Such a macrocyclization strategy embodies the post-translational modification logic of RiPP natural products while appropriating chemical intermediates produced by polyketide synthase modules.

Here, we report that linear peptides with a reactive *N*-terminal  $\beta$ -keto amide functionality can be synthesized ribosomally using in vitro translation (IVT), and that peptides carrying an *N*-terminal  $\beta$ -keto amide are substrates for Friedländer reactions capable of generating a diverse set of quinoline-peptide hybrid products. Reaction of the *N*-terminal  $\beta$ -keto amide with an appropriately substituted 2-aminobenzophenone provides a Friedländer product possessing a stable atropisomeric axis whose structure could be characterized by NMR and X-ray crystallography. Finally, synthetic or IVT peptides carrying both an *N*-terminal  $\beta$ -keto amide and an internal kynurenine residue are substrates for intramolecular Friedländer macrocyclization reactions that embed a quinoline pharmacophore into the peptide backbone. The introduction of simple ketide building blocks into ribosomal synthesis and their post-translational derivatization with carbonyl chemistry expands the structural and stereochemical diversity available to genetically encoded peptides and provides a paradigm for the programmed synthesis of peptide-derived materials that more closely resemble complex natural products.

## Results

### Introduction of a reactive 1,3-dicarbonyl motif at the *N*-terminus via in vitro translation

We began by exploring the extent to which tRNAs could be acylated with monomers carrying a reactive dicarbonyl motif, and the extent to which these acylated tRNAs could initiate the in vitro translation of short peptides (**Fig. 1a**). *N*-formyl methionine (**fm**) and monomers **1-4** (**Fig. 1b**) were converted into activated 3,5-dinitrobenzyl (DNB) esters (**Supplementary Fig. 1a**) and their ability to acylate a model tRNA microhelix (MH, **Supplementary Fig. 2a and Supplementary Table 1**) in the presence of flexizyme dFx<sup>40</sup> was evaluated as a function of time and pH. The extent of MH acylation was monitored using both acidic polyacrylamide gel electrophoresis (aPAGE) (**Supplementary Fig. 2b**) and intact tRNA LC-MS<sup>39,41</sup> (**Supplementary Fig. 2c-g**). Although gel electrophoresis failed to resolve any acylated MH product from the non-acylated MH substrate, presumably due to similarity in mass and charge, intact tRNA LC-MS revealed that both **2-DNB** and **3-DNB** were substrates for dFx in MH-acylation reactions, especially at higher pH and longer incubation times (**Supplementary Table 1**). It is likely that the activity of **3-DNB** as a substrate for dFx was previously missed because of the low resolving power of gel electrophoresis<sup>42</sup>. Although we were unable to identify conditions that led to detectable MH acylation by the 3,5-dinitrobenzyl ester of monomer **1** (**Fig. 1b**), in the case of monomer **4**, intact tRNA LC-MS detected formation of acylated MH in 0.6% yield (**Supplementary Fig. 2g and**

**Supplementary Table 1).** In vitro-transcribed *E. coli* initiator tRNA (tRNA<sup>fMet</sup>) was subsequently acylated on a preparative scale with the 3,5-dinitrobenzyl esters of monomers **2** and **3**; in each case, product identity was confirmed using intact tRNA LC-MS (**Fig. 1c-e**).

With acylated tRNA<sup>fMet</sup> in hand, we next evaluated the extent to which monomers **2** and **3** could be introduced at the *N*-termini of short peptides prepared using in vitro translation (IVT). We made use of a commercial IVT kit (PURExpress<sup>®</sup> Δ (aa, tRNA) Kit), supplemented with the requisite amino acids and tRNAs, tRNA<sup>fMet</sup> pre-acylated with **fM** or monomers **2** or **3**, and a duplex DNA template encoding the FLAG-containing polypeptide MGVDYKDDDDK (MGV-flag). Peptides initiated with monomers **2** or **3** were translated at levels comparable to those initiated with tRNA<sup>fMet</sup> that had been pre-acylated with *N*-formyl methionine (**fM**) (**Fig. 1f-h** and **Supplementary Fig. 3**).

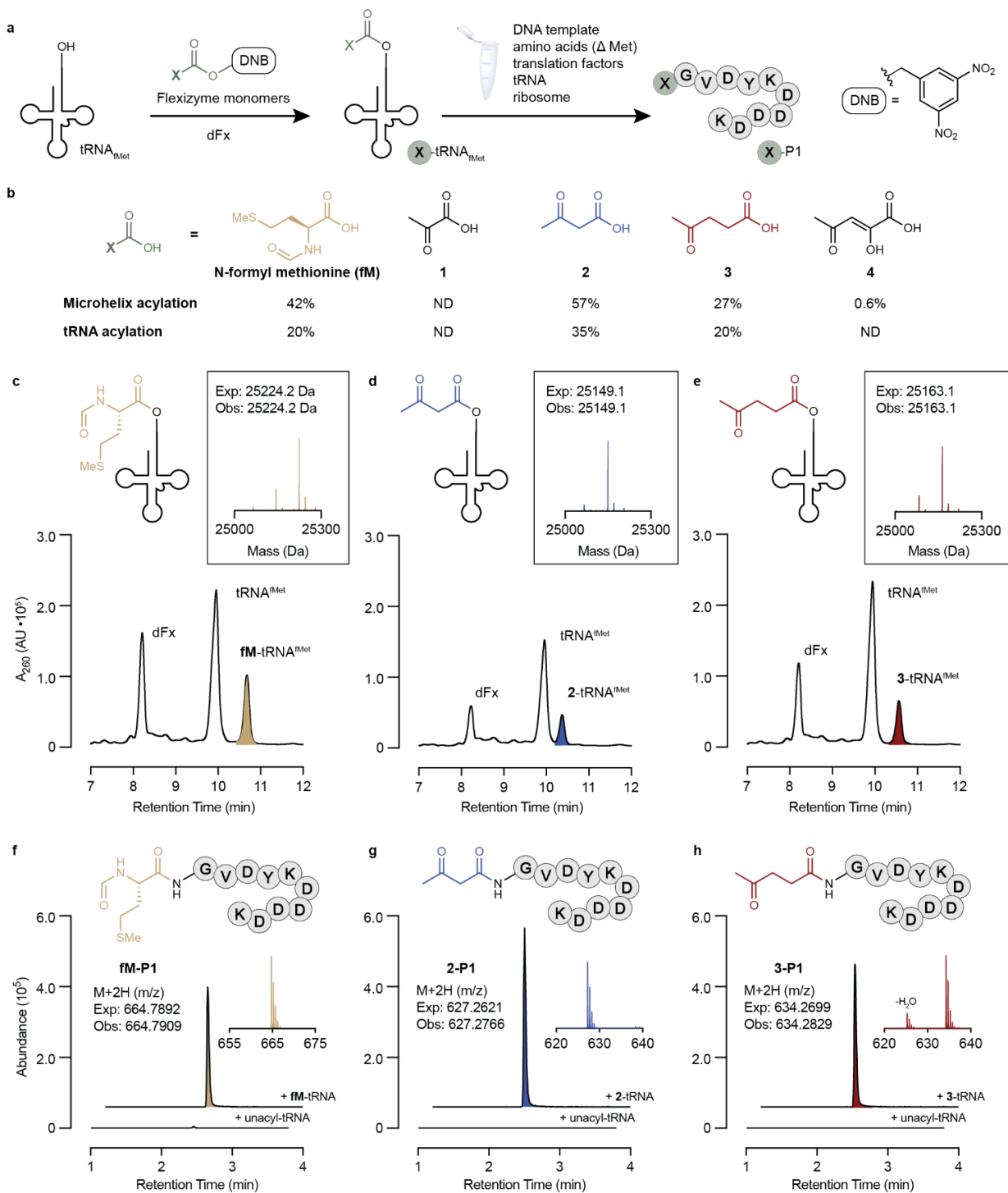


**Figure 1. Introduction of a reactive 1,3-dicarbonyl motif at the N-terminus via in vitro translation.** **a**, Scheme illustrating dFx-promoted acylation of  $\text{tRNA}^{\text{Met}}$  with 3,5-dinitrobenzyl (DNB) esters and use of these tRNAs to initiate the in vitro translation of peptide **P1**, **XGVDYKDDDDK**, where **X** represents *N*-formyl methionine (**fM**) or monomers **1-4**. **DYKDDDDK** is a FLAG-tag that enables peptide isolation and enrichment prior to LC-HRMS analysis. **b**, Yields for flexizyme-promoted acylation of **X** MH and  $\text{tRNA}^{\text{Met}}$  by the DNB esters of **fM** and

monomers **1-4**. Yields were determined using intact tRNA LC-MS<sup>39,41</sup>. ND indicates that an acylated product was not detected. A<sub>260</sub> chromatograms and deconvoluted mass spectra (inset box) of tRNA<sup>fMet</sup> acylated with the DNB esters of **c**, fM (**fM-DNB**), **d**, monomer **2 (2-DNB)**, and **e**, monomer **3 (3-DNB)**. Extracted ion chromatograms of peptide **P1** containing the *N*-terminal residue **f**, **fM**, **g**, **2**, or **h**, **3** in the presence of acylated or non-acylated tRNA<sup>fMet</sup>. The inset shows the mass spectrum of each peptide. All acylations were performed in triplicate. Data shown is representative.

### Friedländer reactions of $\beta$ -keto amides proceed readily under mild aqueous conditions

$\beta$ - and  $\gamma$ -keto carbonyl groups participate in an array of chemical transformations that generate carbocyclic and heterocyclic frameworks, often with elements of stereocontrol<sup>43-45</sup>. One classic transformation is the Friedländer reaction<sup>46</sup>, a double condensation of a 2-aminoarylcarbonyl and an aldehyde or ketone to form a quinoline, a fused [6,6] heterocyclic aromatic ring. Friedländer reactions are typically performed under harsh conditions, requiring a strongly acidic or basic additive and/or reaction temperatures greater than 150 °C (**Fig. 2a**)<sup>47,48</sup>; these conditions would likely degrade sensitive peptides. Although we were encouraged by several reports of high-yielding Friedländer reactions of  $\beta$ -ketoesters performed in acetic acid<sup>49</sup> and acetic acid/water mixtures<sup>50</sup>, we could identify only limited literature examples of Friedländer reactions of  $\beta$ -keto amides<sup>51-54</sup>, and none that proceeded under mild conditions that would be appropriate for peptides and with a wide substrate scope.

We thus sought to identify mild conditions that would support the Friedländer reaction of model  $\beta$ -keto amide **5** (**Fig. 2b**, **Supplementary Fig. 1b**), and apply these conditions to peptides generated using IVT. We examined the reaction of **5** with 2-aminoacetophenone **6** to generate quinoline **15** in acetic acid and acetic acid/water mixtures at temperatures between RT and 60 °C. Reactions were performed using 330 mM of **5** and **6** and the formation of quinoline **15** was monitored as a function of time using LC-MS (**Fig. 2c**). We found that all conditions tested supported the Friedländer reaction of  $\beta$ -keto amide **5** to generate the expected quinoline product **15**. Conversion was most rapid at 60 °C in AcOH or H<sub>2</sub>O/AcOH mixtures or at 40 °C in AcOH (**Fig. 2c**). To evaluate reaction scope under these conditions, we treated  $\beta$ -keto amide **5** with a collection of nine structurally diverse 2-aminoarylcarbonyl substrates **6-14** (**Fig. 2d** and **Supplementary Fig. 4**). Substrates **6** and **9-13** reacted cleanly with  $\beta$ -keto amide **5** with full conversion to the expected quinoline products **15** and **18-22** after 48 h at 60 °C in AcOH. Reactions with 2-aminobenzaldehydes **7** and **8**, which polymerize under acidic conditions<sup>55</sup>, and kynurenine **14**, led to lower levels of product formation (**Supplementary Fig. 5**). Quinolines **15-20** were synthesized on a preparative scale and the products were characterized using LC-HRMS and NMR.

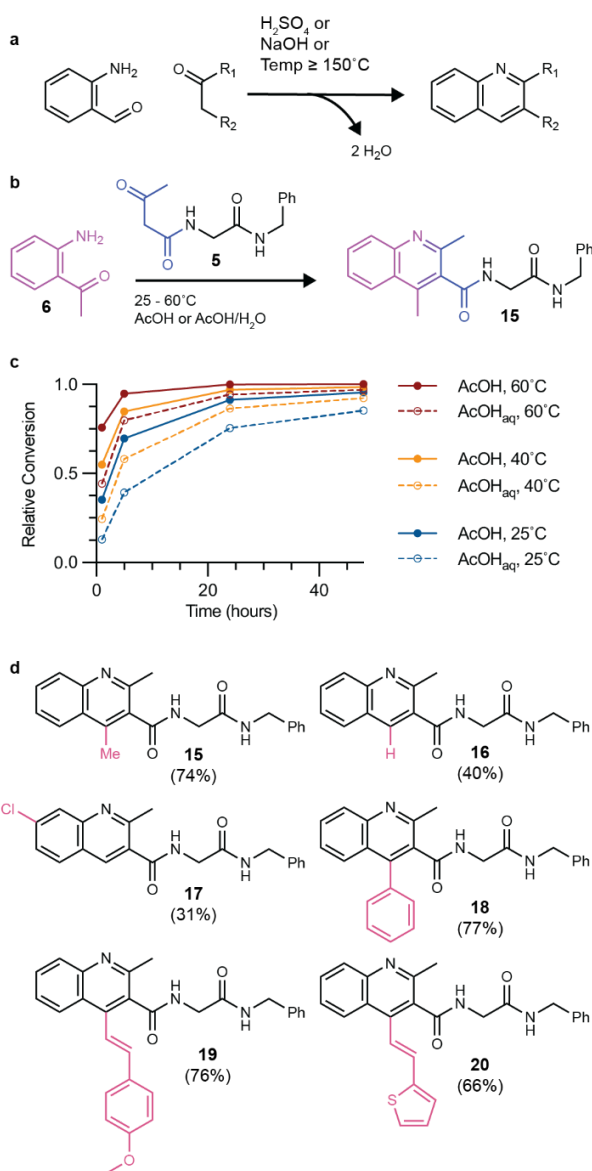


## Figure 2. Friedländer reactions of $\beta$ -keto amides proceed readily in aqueous acetic acid.

**a**, Scheme illustrating a classic Friedländer reaction between 2-aminobenzaldehyde and a substituted ketone. **b**, Model system used to evaluate more mild conditions for the Friedländer reaction of  $\beta$ -keto amide dipeptide **5** and 2-aminoacetophenone **6** (0.33 M each). **c**, Plot illustrating the conversion of **5** and **6** into quinoline **15** under the conditions shown. Relative conversion (RC) values were calculated according to the equation  $RC = [A_{15}/(A_5 + A_{15})]$  where  $A_x$  represents the integrated area of the peaks corresponding to substrate **5** ( $A_5$ ) or product **15** ( $A_{15}$ ) on the absorbance chromatogram (214 nm). Each point represents the average of two replicates. **d**, Representative substituted quinoline products generated from Friedländer reactions performed in AcOH at 60 °C for 48 h. Isolated yields are shown in parentheses; corresponding LC-MS traces are shown in **Supplementary Fig. 5**.

## Post-translational Friedländer reactions of IVT products proceed under mild conditions

We next asked whether Friedländer reactions would also proceed efficiently when performed on IVT peptides initiated with

tRNA<sup>fMet</sup> acylated with monomer **2**. Performing reactions on in vitro translation products is challenging because the reaction must proceed cleanly at low peptide concentration (< 1  $\mu$ M) and in the presence of high concentrations of biomolecules and salts.  $\beta$ -keto amide peptide **2-P1** was generated using IVT, isolated using anti-FLAG magnetic beads, lyophilized, and treated with 2-aminoarylcarbonyl substrates **6**, **8**, **9**, or **12** in acetic acid at 40 °C for 24 h. The formation of Friedländer products **Q6-P1**, **Q8-P1**, **Q9-P1**, and **Q12-P1** were monitored using LC-HRMS (**Supplementary Fig. 6a-d**). In each case, the post-translational Friedländer reaction of **2-P1** proceeded to generate peptides with quinoline derivatives at their N-termini (**Fig. 3b-e**). In theory, identical quinoline-peptide hybrids could be prepared ribosomally using tRNA<sup>fMet</sup> acylated with a pre-assembled quinoline. Yet treatment of tRNA<sup>fMet</sup> with eFx and dimethyl quinoline cyanomethyl ester **25-CME** (**Supplementary Fig. 7a**) led to no detectable acyl-tRNA

product under any condition tested (**Fig. 3f** and **Supplementary Table 2**). We conclude that post-translational Friedländer reactions represent a simple path to ribosomally synthesized peptides with diverse quinoline functionality at the *N*-terminus.

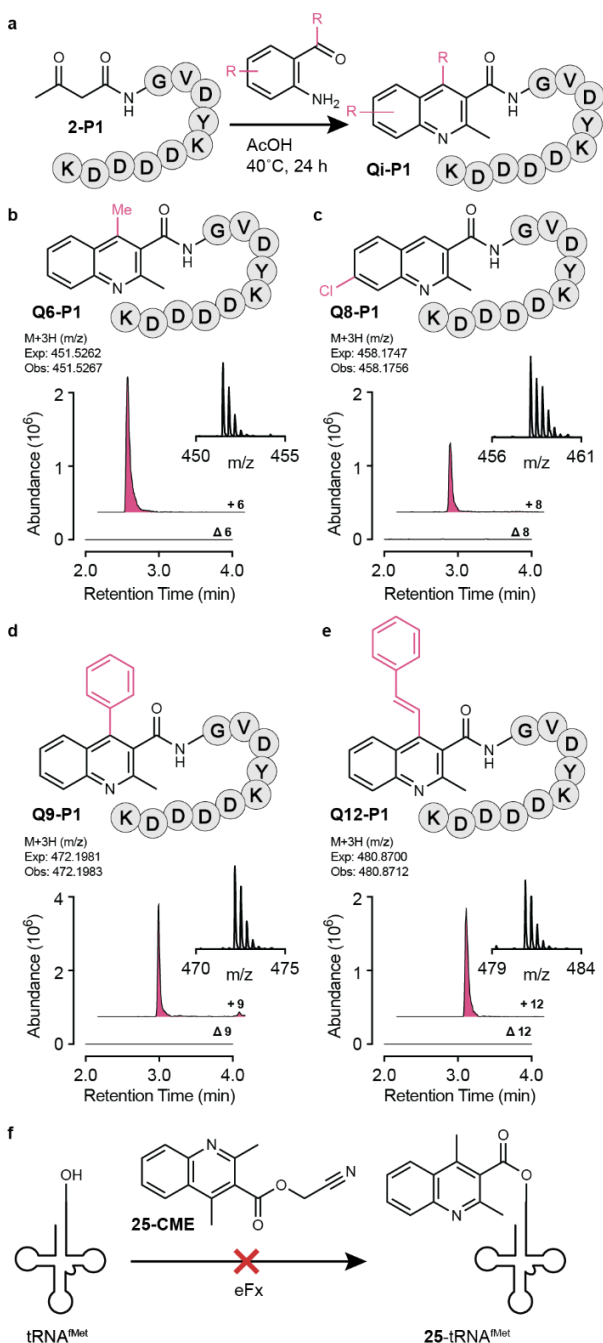


### Figure 3. Post-translational Friedländer reactions on IVT products proceed under mild conditions.

**a**, Post-translational Friedländer reactions of IVT peptide **2-P1** generate diverse quinoline-peptide hybrid molecules **Qi-P1**, where **i** identifies the 2-aminocarbonyl substrate. **b-e**, Reaction scope. Shown is the extracted ion chromatogram (EIC) for the expected major ion produced when **2-P1** is treated under the conditions shown in the presence and absence of substrates **6**, **8**, **9**, or **12** to generate **Q6-P1**, **Q8-P1**, **Q9-P1**, and **Q12-P1**, respectively. The mass spectrum of each major ion is inset. **f**, eFx-promoted acylation of tRNA<sup>fMet</sup> with quinoline cyanomethyl ester **25-CME** led to no detectable acylated tRNA product under any condition tested.

### Friedländer reactions of $\beta$ -keto amides generate stable atropisomers

Appropriately substituted quinolines can exist as atropisomers. Canonical atropisomers are stereoisomers that arise from hindered rotation around a  $\sigma$ -bond<sup>56</sup>. Like stereoisomers with point chirality, atropisomers can bind macromolecular targets with distinct kinetics as well as different affinities<sup>57</sup>. Atropisomeric quinolines and quinoline-like heterocycles are well known. They are found in pharmaceuticals<sup>58–60</sup> such as Sotorasib, a first-in-class mutant KRAS G12C inhibitor<sup>58,59</sup>, as well as novel HIV-I integrase inhibitors<sup>63</sup>. Atropisomeric quinolines also serve as the molecular

framework for catalysts with widespread use in organic synthesis and process research, such as QUINAP<sup>58</sup>. Although many macrocyclic peptide natural products contain unusual structural isomers, sometimes called atropisomers<sup>64</sup>, non-canonical atropisomers<sup>65</sup>, or ansamers<sup>66</sup>, that result from threaded-loop or knot-like structures<sup>65,67,68</sup>, true canonical atropisomers are also

important constituents of this class of compounds, such as the famous case of the cyclic glycopeptide vancomycin<sup>69</sup>. Peptides or cyclic peptides containing atropisomeric quinolines would add a sophisticated layer of stereochemical complexity to macrocyclic peptide libraries.

To assess whether atropisomeric quinolines could be introduced within ribosomal peptides, we first confirmed that Friedländer reaction of peptide **28** with (2-aminophenyl)(*o*-tolyl)methanone (**26**) in AcOH at 60 °C for 48 h produced the expected product **29** as a roughly 41:59 mixture of atropisomeric products, as determined by <sup>1</sup>H NMR (Fig. 4a). However, when we attempted to reproduce a post-translational Friedländer reaction between (2-aminophenyl)(*o*-tolyl)methanone (**26**) and IVT-generated peptide **2-P1** in acetic acid, the expected product **Q26-P1** was detected, but in low abundance (Fig. 4c).

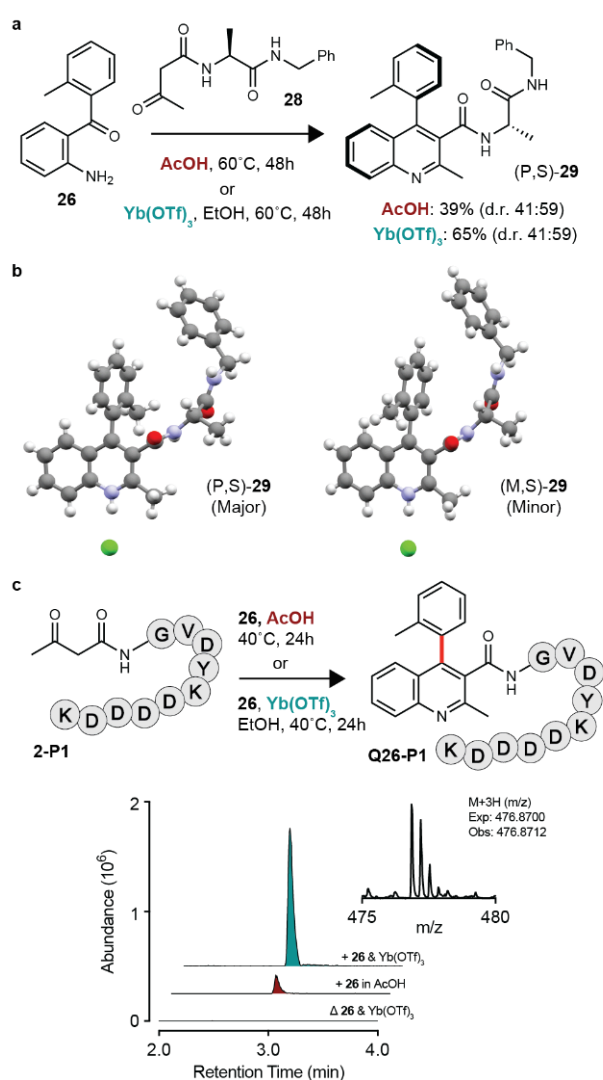


**Figure 4. Friedländer reactions of  $\beta$ -keto amides generate stable atropisomers. a**, Friedländer reaction of substrate **26** and dipeptide **28** in the presence of either Brønsted or Lewis acids generates quinoline-dipeptide **29**, which exists as a pair of stable atropisomers with a diastereomeric ratio (d.r.) of ~41:59 regardless of the conditions used for its preparation. **b**, X-ray crystal structure of (*P*, *S*)-**29** (left, CCDC: 2341553) and (*M*, *S*)-**29** (right, CCDC: 2341552) as their respective hydrochloride salts. **c**, Friedländer reaction of **2-P1**, prepared using IVT, with aminocarbonyl **26** in the presence of 100 mM Yb(OTf)<sub>3</sub> in EtOH generates quinoline-peptide **Q26-P1**. Extracted ion chromatograms for product formation in the presence of Yb(OTf)<sub>3</sub> in EtOH with **26** (teal), acetic acid with **26** (red), or Yb(OTf)<sub>3</sub> in EtOH without **26** (black) for 24 h at 40 °C. Significantly less product is observed when the reaction is performed using AcOH in place of Yb(OTf)<sub>3</sub> in EtOH.

#### Lewis acid catalysis of post-translational Friedländer reactions generates atropisomeric products

We hypothesized that Friedländer reactions of  $\beta$ -keto amide-containing peptides could be optimized using mild Lewis acid-catalyzed conditions, thus allowing for good reactivity with ribosomal peptides generated by IVT. Indeed, Lewis acids such as the chloride salts of Ce(III)<sup>70</sup> and Fe(III)<sup>71</sup> as well as the triflate salts of

Yb(III)<sup>72</sup>, Y(III)<sup>73</sup>, and Zn(II)<sup>74</sup>, can promote Friedländer reactions of  $\beta$ -ketoesters<sup>48</sup>. To evaluate if they could improve atropisomer-forming reactions of  $\beta$ -keto amide **2-P1**, we screened their effect (at 20 mol%) on the Friedländer reaction of dipeptide **5** and (2-aminophenyl)(*o*-tolyl)methanone (**26**) to generate the quinoline **27** (**Supplementary Fig. 9** and **Supplementary Table 3**). Of all Lewis acids tested, the highest yields were obtained with Yb(OTf)<sub>3</sub> in ethanol. Yb(OTf)<sub>3</sub> was versatile, performing well in DCM, MeCN, THF, and AcOH. Although strong Brønsted acids such as triflic acid, sulfuric acid, phosphoric acid, and trifluoroacetic acid also out-performed acetic acid, these conditions are far less mild. When the Friedländer reaction of **28** and **26** was repeated, this time in the presence of 20 mol% Yb(OTf)<sub>3</sub> in EtOH at 60 °C for 48 h, we isolated the product **29** in 65% yield with a similar diastereomeric ratio (**Fig. 4a**). The diastereomers could be separated and subsequently characterized by <sup>1</sup>H NMR (**Supplementary Fig. 8**) and X-ray structure determination (**Fig. 4b, Supplementary Fig. 10 & 11, and Supplementary Tables 4 & 5**), revealing that the (*P*, *S*) diastereomer is the major product. The stability of the atropisomeric axis was assessed by heating a pure sample of the minor diastereomer (i.e., (*M*, *S*)-**29**) in DMSO-*d*<sub>6</sub> at 100 °C for 18 h<sup>75</sup>. Subsequent <sup>1</sup>H NMR analysis revealed minimal epimerization (< 1%, **Supplementary Fig. 12**). With optimized conditions in hand, we again attempted modification of a ribosomal peptide generated by IVT. Indeed, when treated with **26** in EtOH containing Yb(OTf)<sub>3</sub>, the IVT synthesized  $\beta$ -keto amide peptide **2-P1** was transformed cleanly into the quinoline-peptide hybrid **Q26-P1** after 24 h at 40 °C (**Fig. 4c and Supplementary Fig. 6e**). **Q26-P1** is presumed to exist as a mixture of atropisomers in analogy to **29**, but chromatographic separation of distinct isomers by reverse phase UPLC-MS was not observed on this larger IVT peptide.

### Friedländer macrocyclizations

We envisioned that Lewis acids might also aid post-translational Friedländer macrocyclization reactions to generate products with a quinoline pharmacophore embedded within the peptide backbone. To test this idea, we prepared four linear peptides containing both an *N*-terminal  $\beta$ -keto amide and an internal 2-aminoarylcarbonyl side chain provided by the non-canonical amino acid kynurenine (**Fig. 5a and Supplementary Fig. 13-15**). The linear peptide **LP1** is a heptapeptide related to the FDA-approved drug octreotide<sup>5,76</sup>, while **LP2** is a hexapeptide containing a turn-inducing L-proline, **LP3** is a decapeptide bearing diverse functional groups, and **LP4** is a longer diverse tridecapeptide related to the hormone somatostatin<sup>77</sup>. All four linear peptides **LP1-4** (1 mM) underwent intramolecular Friedländer reactions to generate macrocycles **CP1-4** (**Supplementary Fig. 16**) in the presence of 1-2 mM Yb(OTf)<sub>3</sub> in EtOH or MeCN at 60 °C, as supported by LC-HRMS (**Fig. 5b-e and Supplementary Fig. 17-20**) and NMR experiments (**Supplementary Fig. 21 and 23 and Supplementary Data**). The smaller peptides **LP1** and **LP2** cyclized cleanly and the macrocyclic products **CP1** and **CP2** could be isolated with efficiencies that tracked well with LC-MS and HPLC chromatograms of reaction progress. **CP1** and **CP2** were isolated as salts in complex with TFA employed in the isolation procedure (see **Supplementary Material**). Cyclization of the larger peptides **LP3** and **LP4** proceeded under analogous conditions to deliver their corresponding macrocycles with reduced, but still notable efficiency. For comparison, macrocyclization reactions of **LP1-4** were also performed under aqueous conditions (80 mM glycine pH 2.8 at 60 °C); in all cases, cyclization proceeded

faster using the Lewis acid  $\text{Yb}(\text{OTf})_3$  (**Supplementary Fig. 24**). The isolated macrocycles **CP1-CP4** were also characterized by MALDI-TOF MS to confirm the monomeric mass and the absence of significant quantities of higher order oligomers (**Supplementary Fig 25 and Supplementary Data**).

Finally we asked whether a Lewis acid-catalyzed Friedländer macrocyclization reaction was compatible with the challenging conditions required for post-translational modifications of in vitro translation (IVT) products. First, the cyanomethyl ester of kynurenine (**Kyn-CME**) and the flexizyme eFx were used to acylate  $\text{tRNA}^{\text{AsnE2\#2}}_{\text{GCU}}$ , a previously reported engineered  $\text{tRNA}^{\text{78}}$  (**Supplementary Figs. 7b & 26**). The resulting Kyn- $\text{tRNA}^{\text{AsnE2\#2}}_{\text{GCU}}$  was added to the IVT reaction while excluding serine and sequestering native  $\text{tRNA}^{\text{Ser}}_{\text{GCU}}$  with an antisense oligonucleotide (M5-1) to suppress near cognate read-through<sup>26,79</sup>. We confirmed that  $\beta$ -ketoacid **2** and kynurenine (**Kyn**) could independently and effectively recode methionine at position 1 and serine at position 6, respectively, of a peptide prepared using IVT (**Supplementary Fig. 27**). Using an identical strategy, we then used IVT to generate tetraikadeca peptide **ivt.LP5**, which contains both an *N*-terminal  $\beta$ -keto amide as well as an internal kynurenine residue (**Fig. 5f**). Subsequent reaction of **ivt.LP5** with 100 mM  $\text{Yb}(\text{OTf})_3$  in MeCN at 60 °C for 24 h yielded quinoline-cyclized peptide **ivt.CP5** (**Fig. 5f,g**) whose retention time and mass spectrum were identical to that of an authentic standard produced by SPPS (**Supplementary Fig. 27**). This result confirms that mild, post-translational Lewis acid-catalyzed Friedländer reactions can effectively generate macrocyclic quinoline-peptide hybrids even at very low peptide concentrations and in the presence of the high concentrations of salts and biomolecules that are intrinsic to in vitro translation reactions.

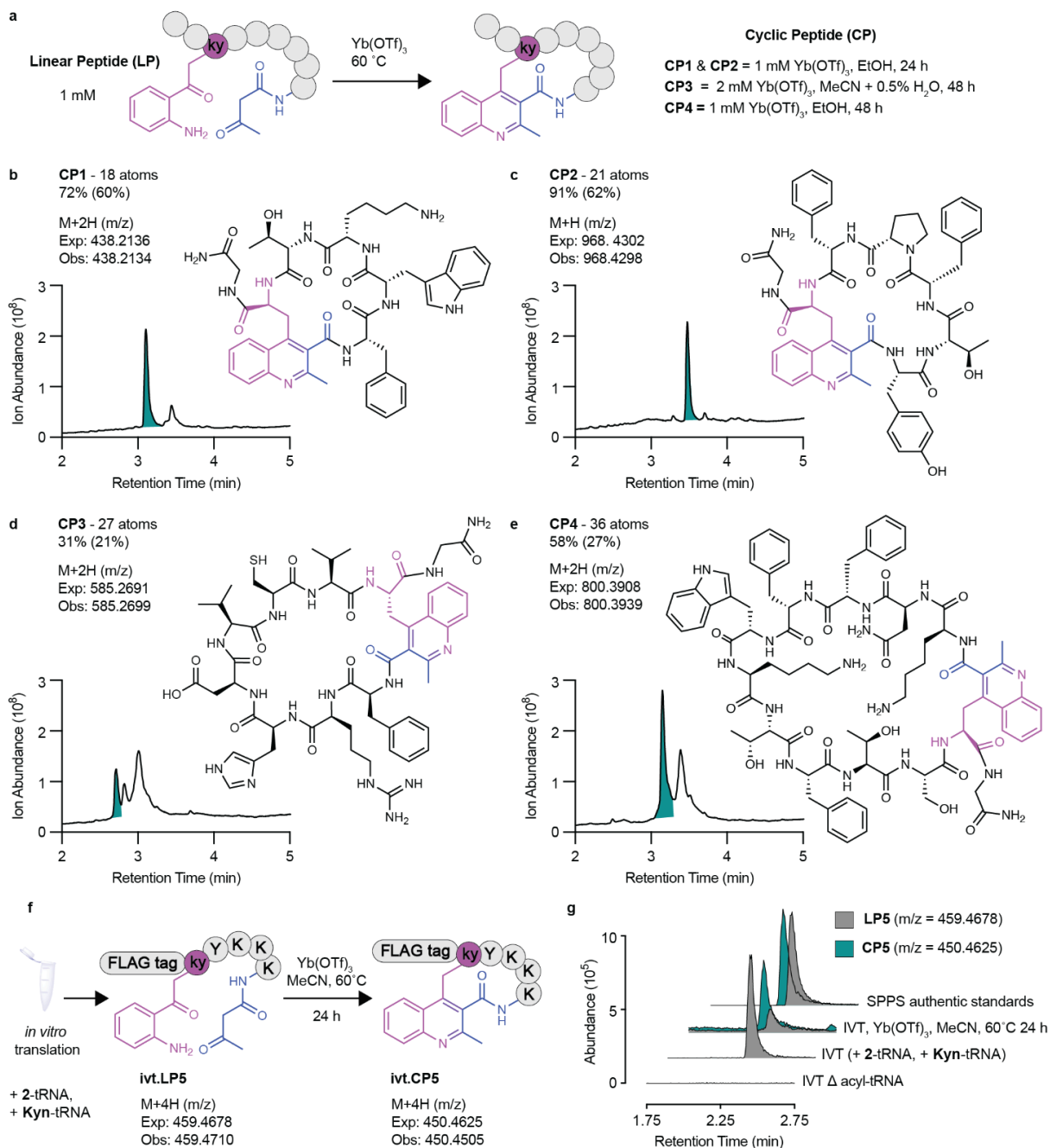


**Fig. 5. Intramolecular post-translational Friedländer macrocyclization reactions.** **a**, Preparative scale intramolecular Friedländer reactions to generate peptide macrocycles with an embedded backbone quinoline. Each linear peptide contains monomer **2** at the *N*-terminus and a single internal kynurenine residue. **b-e**, Structures and total ion chromatograms of crude reaction mixtures for synthetic peptides **CP1-4** after Friedländer macrocyclization reactions. The peak containing the cyclic peptide is highlighted in teal. Atom count of the macrocycle backbone, HPLC<sub>254nm</sub> yield, and isolated yield (in parentheses) are provided. All peptides were prepared using solid phase methods and purified as described in **Supplementary Methods**.

Detailed synthetic information, including LC-HRMS, MS-MS, and NMR of linear and cyclic peptides can be found in **Supplementary Fig. 13-25. f**, Incorporation of both **2** and **Kynurenine** into a single IVT peptide **ivt.LP5** and subsequent Friedländer cyclization into **ivt.CP5. g**, Extracted ion chromatograms of **ivt.LP5** and **ivt.CP5** and comparison with an authentic standard prepared using solid phase methods.

## Discussion

Peptides and their derivatives are a rapidly expanding class of therapeutic molecules, in part because they condense the expansive recognition properties of a protein into a more compact molecular framework. The extended binding surface of a peptide provides a better complement to the extended and featureless surfaces that comprise many traditionally “undruggable” targets<sup>80</sup>. Perhaps the greatest attribute of peptides, whether linear or cyclic, is that they are genetically encodable, and hence their properties can be optimized using directed evolution methods performed *in vitro* or *in vivo*. Many of these methods depend on ribosomal translation and reliably return peptide leads for challenging and clinically relevant targets. For these reasons, *de novo* peptides have attracted significant attention as the next frontier in pharmaceutical development<sup>81</sup>.

Yet the difference between the *de novo* peptide lead and the final compound advanced to clinical trials is often profound, and the modifications introduced demand exceptional commitments of labor and state-of-the-art medicinal chemistry<sup>82</sup>. Introducing these modifications earlier in the discovery process would be advantageous. Some important progress has been made, including the introduction of *N*-Me groups<sup>83</sup>, D-amino acids<sup>84</sup>,  $\beta^2$ - and  $\beta^3$ -amino acids, as well as linkers that introduce rings<sup>7</sup> or even appended pharmacophores<sup>25,28</sup>. Even with these developments, the chemistry available to ribosomally translated-peptides remains limited when compared to the vast array of transformations, functional groups, and architectures that are emblematic of small molecule pharmaceuticals and bioactive natural products. Yudin and others have shown that the introduction of heterocyclic grafts into peptide macrocycles can have profound impacts on passive permeability, bioavailability, and even topological complexity<sup>85,86</sup>. Quinolines, however, are underrepresented among these grafts; thus, the properties imbued by these motifs represent an area ripe for further exploration.

This work was initiated in an attempt to generate ribosomally synthesized peptides with modifications that resemble those found in peptide-derived clinical candidates. We accomplished this goal by installing a reactive  $\beta$ -keto amide functional group at the *N*-terminus and developing mild Friedländer reaction conditions to convert the  $\beta$ -keto amide into quinoline-peptide hybrids, including those that exist in distinct atropisomeric forms. The same mild Friedländer conditions were deployed as a macrocyclization strategy, embedding a quinoline pharmacophore directly into the backbone of a sequence-encoded macrocycle.

Finally we note the *N*-terminal  $\beta$ -keto amide and  $\gamma$ -keto amide peptides generated are suitable substrates for many other macrocyclization or late-stage diversification reactions<sup>44</sup>. Potential reactions of *N*-terminal  $\beta$ - and  $\gamma$ -keto amides include those that generate pyridines (Hantzsch

reaction<sup>87</sup>), pyrazoles (Knorr<sup>88</sup>), pyrroles (Hantzsch, Knorr, Paal-Knorr<sup>89</sup>), dihydropyrimidinones (Biginelli<sup>90</sup>), and carbocycles (Conia-Ene<sup>91</sup>), in addition to Michael additions, alkylations, acylations, and arylations. Some of these reactions also have the potential to install atropisomeric axes into the macrocyclic product. These modifications could be used alone or combined with more traditional backbone diversification strategies to generate biased libraries containing pharmacophores and drug-like motifs. We envision the ribosomal incorporation of  $\beta$ - and  $\gamma$ -keto amides as an important development in the late-stage functionalization and macrocyclization of peptides with validated drug-like features.

## References cited

1. Sims, E. K., Carr, A. L. J., Oram, R. A., DiMeglio, L. A. & Evans-Molina, C. 100 years of insulin: celebrating the past, present and future of diabetes therapy. *Nat. Med.* **27**, 1154–1164 (2021).
2. Banting, F. G., Best, C. H., Collip, J. B., Campbell, W. R. & Fletcher, A. A. Pancreatic Extracts in the Treatment of Diabetes Mellitus. *Can. Med. Assoc. J.* **12**, 141–146 (1922).
3. Wilding, J. P. H. *et al.* Once-Weekly Semaglutide in Adults with Overweight or Obesity. *N. Engl. J. Med.* **384**, 989–1002 (2021).
4. Müller, T. D., Blüher, M., Tschöp, M. H. & DiMarchi, R. D. Anti-obesity drug discovery: advances and challenges. *Nat. Rev. Drug Discov.* **21**, 201–223 (2022).
5. Muttenthaler, M., King, G. F., Adams, D. J. & Alewood, P. F. Trends in peptide drug discovery. *Nat. Rev. Drug Discov.* **20**, 309–325 (2021).
6. Costa, L., Sousa, E. & Fernandes, C. Cyclic Peptides in Pipeline: What Future for These Great Molecules? *Pharmaceuticals* **16**, 996 (2023).
7. Zorzi, A., Deyle, K. & Heinis, C. Cyclic peptide therapeutics: past, present and future. *Curr. Opin. Chem. Biol.* **38**, 24–29 (2017).
8. Yang, J. *et al.* Utilization of macrocyclic peptides to target protein-protein interactions in cancer. *Front. Oncol.* **12**, (2022).
9. Ohta, A. *et al.* Validation of a New Methodology to Create Oral Drugs beyond the Rule of 5 for Intracellular Tough Targets. *J. Am. Chem. Soc.* (2023) doi:10.1021/jacs.3c07145.
10. Tucker, T. J. *et al.* A Series of Novel, Highly Potent, and Orally Bioavailable Next-Generation Tricyclic Peptide PCSK9 Inhibitors. *J. Med. Chem.* **64**, 16770–16800 (2021).
11. Li, X., Craven, T. W. & Levine, P. M. Cyclic Peptide Screening Methods for Preclinical Drug Discovery. *J. Med. Chem.* **65**, 11913–11926 (2022).
12. Sawyer, T. Entrepreneurial Drug Hunter: Macrocyclic Peptide Modalities. in

- Contemporary Accounts in Drug Discovery and Development* (eds. Huang, X., Aslanian, R. G. & Tang, W. H.) 273–292 (Wiley, 2022). doi:10.1002/9781119627784.ch12.
13. Howard, J. F. *et al.* Safety and efficacy of zilucoplan in patients with generalised myasthenia gravis (RAISE): a randomised, double-blind, placebo-controlled, phase 3 study. *Lancet Neurol.* **22**, 395–406 (2023).
  14. Rezai, T., Yu, B., Millhauser, G. L., Jacobson, M. P. & Lokey, R. S. Testing the Conformational Hypothesis of Passive Membrane Permeability Using Synthetic Cyclic Peptide Diastereomers. *J. Am. Chem. Soc.* **128**, 2510–2511 (2006).
  15. Rossi Sebastiano, M. *et al.* Impact of Dynamically Exposed Polarity on Permeability and Solubility of Chameleonic Drugs Beyond the Rule of 5. *J. Med. Chem.* **61**, 4189–4202 (2018).
  16. He, J., Ghosh, P. & Nitsche, C. Biocompatible strategies for peptide macrocyclisation. *Chem. Sci.* **15**, 2300–2322 (2024).
  17. White, C. J. & Yudin, A. K. Contemporary strategies for peptide macrocyclization. *Nat. Chem.* **3**, 509–524 (2011).
  18. Bechtler, C. & Lamers, C. Macrocyclization strategies for cyclic peptides and peptidomimetics. *RSC Med. Chem.* **12**, 1325–1351 (2021).
  19. Miller, S. J., Blackwell, H. E. & Grubbs, R. H. Application of Ring-Closing Metathesis to the Synthesis of Rigidified Amino Acids and Peptides. *J. Am. Chem. Soc.* **118**, 9606–9614 (1996).
  20. Walensky, L. D. & Bird, G. H. Hydrocarbon-Stapled Peptides: Principles, Practice, and Progress. *J. Med. Chem.* **57**, 6275–6288 (2014).
  21. Rivera, D. G., Ojeda-Carralero, G. M., Reguera, L. & Eycken, E. V. V. der. Peptide macrocyclization by transition metal catalysis. *Chem. Soc. Rev.* **49**, 2039–2059 (2020).
  22. Passioura, T. The Road Ahead for the Development of Macrocyclic Peptide Ligands. *Biochemistry* **59**, 139–145 (2020).
  23. Melsen, P. R. A., Yoshisada, R. & Jongkees, S. A. K. Opportunities for Expanding

- Encoded Chemical Diversification and Improving Hit Enrichment in mRNA-Displayed Peptide Libraries. *ChemBioChem* **23**, e202100685 (2022).
24. Smolyar, I. V., Yudin, A. K. & Nenajdenko, V. G. Heteroaryl Rings in Peptide Macrocycles. *Chem. Rev.* **119**, 10032–10240 (2019).
  25. Iskandar, S. E. *et al.* Enabling Genetic Code Expansion and Peptide Macrocyclization in mRNA Display via a Promiscuous Orthogonal Aminoacyl-tRNA Synthetase. *J. Am. Chem. Soc.* **145**, 1512–1517 (2023).
  26. Liu, M. *et al.* Selective thiazoline peptide cyclisation compatible with mRNA display and efficient synthesis. *Chem. Sci.* (2023) doi:10.1039/D3SC03117A.
  27. Dengler, S. *et al.* Display Selection of a Hybrid Foldamer–Peptide Macrocycle. *Angew. Chem. Int. Ed.* **62**, e202308408 (2023).
  28. Ekanayake, A. I. *et al.* Genetically Encoded Fragment-Based Discovery from Phage-Displayed Macrocyclic Libraries with Genetically Encoded Unnatural Pharmacophores. *J. Am. Chem. Soc.* **143**, 5497–5507 (2021).
  29. Yadav, P. & Shah, K. Quinolines, a perpetual, multipurpose scaffold in medicinal chemistry. *Bioorganic Chem.* **109**, 104639 (2021).
  30. Musiol, R. An overview of quinoline as a privileged scaffold in cancer drug discovery. *Expert Opin. Drug Discov.* **12**, 583–597 (2017).
  31. Childs-Disney, J. L. *et al.* Targeting RNA structures with small molecules. *Nat. Rev. Drug Discov.* **21**, 736–762 (2022).
  32. Costales, M. G., Childs-Disney, J. L., Haniff, H. S. & Disney, M. D. How We Think about Targeting RNA with Small Molecules. *J. Med. Chem.* **63**, 8880–8900 (2020).
  33. Haniff, H. S., Knerr, L., Chen, J. L., Disney, M. D. & Lightfoot, H. L. Target-Directed Approaches for Screening Small Molecules against RNA Targets. *SLAS Discov.* **25**, 869–894 (2020).
  34. Donlic, A. *et al.* R-BIND 2.0: An Updated Database of Bioactive RNA-Targeting Small

- Molecules and Associated RNA Secondary Structures. *ACS Chem. Biol.* **17**, 1556–1566 (2022).
35. Krishnamurthy, M., Gooch, B. D. & Beal, P. A. Peptide Quinoline Conjugates: A New Class of RNA-Binding Molecules. *Org. Lett.* **6**, 63–66 (2004).
  36. Krishnamurthy, M., Simon, K., Orendt, A. M. & Beal, P. A. Macrocyclic Helix-Threading Peptides for Targeting RNA. *Angew. Chem. Int. Ed.* **46**, 7044–7047 (2007).
  37. Chen, J. L. *et al.* Design, Optimization, and Study of Small Molecules That Target Tau Pre-mRNA and Affect Splicing. *J. Am. Chem. Soc.* **142**, 8706–8727 (2020).
  38. Ad, O. *et al.* Translation of Diverse Aramid- and 1,3-Dicarbonyl-peptides by Wild Type Ribosomes *in Vitro*. *ACS Cent. Sci.* **5**, 1289–1294 (2019).
  39. Fricke, R. *et al.* Expanding the substrate scope of pyrrolysyl-transfer RNA synthetase enzymes to include non- $\alpha$ -amino acids *in vitro* and *in vivo*. *Nat. Chem.* **15**, 960–971 (2023).
  40. Murakami, H., Ohta, A., Ashigai, H. & Suga, H. A highly flexible tRNA acylation method for non-natural polypeptide synthesis. *Nat. Methods* **3**, 357–359 (2006).
  41. Fricke, R., Knudson, I. & Schepartz, A. Direct, quantitative, and comprehensive analysis of tRNA acylation using intact tRNA liquid-chromatography mass-spectrometry. 2023.07.14.549096 Preprint at <https://doi.org/10.1101/2023.07.14.549096> (2023).
  42. Lee, J. *et al.* Ribosome-mediated biosynthesis of pyridazinone oligomers *in vitro*. *Nat. Commun.* **13**, 6322 (2022).
  43. Li, W., Zheng, Y., Qu, E., Bai, J. & Deng, Q.  $\beta$ -Keto Amides: A Jack-of-All-Trades Building Block in Organic Chemistry. *Eur. J. Org. Chem.* **2021**, 5151–5192 (2021).
  44. Wu, X. & Li, W. The applications of  $\beta$ -keto amides for heterocycle synthesis. *J. Heterocycl. Chem.* **59**, 1445–1490 (2022).
  45. Amarnath, V. & Amarnath, K. Intermediates in the Paal-Knorr Synthesis of Furans. *J. Org. Chem.* **60**, 301–307 (1995).
  46. Friedlaender, P. Ueber o-Amidobenzaldehyd. *Berichte Dtsch. Chem. Ges.* **15**,

2572–2575 (1882).

47. Cheng, C.-C. & Yan, S.-J. The Friedländer Synthesis of Quinolines. in *Organic Reactions* 37–201 (John Wiley & Sons, Ltd, 2005). doi:10.1002/0471264180.or028.02.
48. Marco-Contelles, J., Pérez-Mayoral, E., Samadi, A., Carreiras, M. & Soriano, E. Recent Advances in the Friedländer Reaction. *Chem. Rev.* **109**, 2652–71 (2009).
49. Meléndez, A. *et al.* Straightforward Synthesis of Novel 4-Styrylquinolines/4-Styrylquinolin-2-ones and 9-Styryldihydroacridin-1(2H)-ones from Substituted 2'-Aminochalcones. *Synthesis* **52**, 1804–1822 (2020).
50. Shen, Q. *et al.* Synthesis of Quinolines via Friedländer Reaction in Water and under Catalyst-Free Conditions. *Synthesis* **44**, 389–392 (2012).
51. Tîrînşaş, M.-L. *et al.* Rational design of carbamate-based dual binding site and central AChE inhibitors by a “biooxidisable” prodrug approach: Synthesis, in vitro evaluation and docking studies. *Eur. J. Med. Chem.* **155**, 171–182 (2018).
52. Atechian, S. *et al.* New vistas in quinoline synthesis. *Tetrahedron* **63**, 2811–2823 (2007).
53. Gopi, P. & Sarveswari, S. Effective water mediated green synthesis of polysubstituted quinolines without energy expenditure. *Monatshefte Für Chem. - Chem. Mon.* **148**, 1043–1049 (2017).
54. Bose, D. S., Idrees, Mohd., Jakka, N. M. & Rao, J. V. Diversity-Oriented Synthesis of Quinolines via Friedländer Annulation Reaction under Mild Catalytic Conditions. *J. Comb. Chem.* **12**, 100–110 (2010).
55. Albert, A. & Yamamoto, H. The structures of the anhydro-polymers of 2-aminobenzaldehyde. *J. Chem. Soc. B Phys. Org.* 956 (1966) doi:10.1039/j29660000956.
56. Christie, G. H. & Kenner, J. LXXI.—The molecular configurations of polynuclear aromatic compounds. Part I. The resolution of  $\gamma$ -6 : 6'-dinitro- and 4 : 6 : 4' : 6'-tetranitro-diphenic acids into optically active components. *J. Chem. Soc. Trans.* **121**, 614–620 (1922).
57. Perreault, S., Chandrasekhar, J. & Patel, L. Atropisomerism in Drug Discovery: A

- Medicinal Chemistry Perspective Inspired by Atropisomeric Class I PI3K Inhibitors. *Acc. Chem. Res.* **55**, 2581–2593 (2022).
58. Basilaia, M., Chen, M. H., Secka, J. & Gustafson, J. L. Atropisomerism in the Pharmaceutically Relevant Realm. *Acc. Chem. Res.* **55**, 2904–2919 (2022).
  59. LaPlante, S. R. *et al.* Assessing Atropisomer Axial Chirality in Drug Discovery and Development. *J. Med. Chem.* **54**, 7005–7022 (2011).
  60. Toenjes, S. T. & Gustafson, J. L. Atropisomerism in medicinal chemistry: challenges and opportunities. *Future Med. Chem.* **10**, 409–422 (2018).
  61. Janes, M. R. *et al.* Targeting KRAS Mutant Cancers with a Covalent G12C-Specific Inhibitor. *Cell* **172**, 578-589.e17 (2018).
  62. Lanman, B. A., Parsons, A. T. & Zech, S. G. Addressing Atropisomerism in the Development of Sotorasib, a Covalent Inhibitor of KRAS G12C: Structural, Analytical, and Synthetic Considerations. *Acc. Chem. Res.* **55**, 2892–2903 (2022).
  63. Fader, L. D. *et al.* Discovery of BI 224436, a Noncatalytic Site Integrase Inhibitor (NCINI) of HIV-1. *ACS Med. Chem. Lett.* **5**, 422–427 (2014).
  64. Nanudorn, P. *et al.* Atropopeptides are a Novel Family of Ribosomally Synthesized and Posttranslationally Modified Peptides with a Complex Molecular Shape. *Angew. Chem.* **n/a**,.
  65. Reisberg, S. H. *et al.* Total synthesis reveals atypical atropisomerism in a small-molecule natural product, tryptorubin A. *Science* **367**, 458–463 (2020).
  66. Yao, G. *et al.* The occurrence of ansamers in the synthesis of cyclic peptides. *Nat. Commun.* **13**, 6488 (2022).
  67. Hegemann, J. D., Zimmermann, M., Xie, X. & Marahiel, M. A. Lasso Peptides: An Intriguing Class of Bacterial Natural Products. *Acc. Chem. Res.* **48**, 1909–1919 (2015).
  68. de Veer, S. J., Kan, M.-W. & Craik, D. J. Cyclotides: From Structure to Function. *Chem. Rev.* **119**, 12375–12421 (2019).
  69. Moore, M. J. *et al.* Next-Generation Total Synthesis of Vancomycin. *J. Am. Chem. Soc.*

- 142**, 16039–16050 (2020).
70. Bose, D. S. & Kumar, R. K. An efficient, high yielding protocol for the synthesis of functionalized quinolines via the tandem addition/annulation reaction of o-aminoaryl ketones with  $\alpha$ -methylene ketones. *Tetrahedron Lett.* **47**, 813–816 (2006).
71. Wu, J., Zhang, L. & Diao, T.-N. An Expedient Approach to Quinolines via Friedländer Synthesis Catalyzed by  $\text{FeCl}_3$  or  $\text{Mg}(\text{ClO}_4)_2$ . *Synlett* 2653–2657 (2005)  
doi:10.1055/s-2005-917111.
72. Muchowski, J. M. & Maddox, M. L. Concerning the mechanism of the Friedländer quinoline synthesis. *Can. J. Chem.* **82**, 461–478 (2004).
73. De, S. K. & Gibbs, R. A. A mild and efficient one-step synthesis of quinolines. *Tetrahedron Lett.* **46**, 1647–1649 (2005).
74. Lekhok, K. C., Bhuyan, D., Prajapati, D. & Boruah, R. C. Zinc triflate: a highly efficient reusable catalyst in the synthesis of functionalized quinolines via Friedlander annulation. *Mol. Divers.* **14**, 841–846 (2010).
75. Shao, Y.-D. *et al.* Organocatalytic Atroposelective Friedländer Quinoline Heteroannulation. *Org. Lett.* **21**, 4831–4836 (2019).
76. Pohl, E. *et al.* Structure of octreotide, a somatostatin analogue. *Acta Crystallogr. D Biol. Crystallogr.* **51**, 48–59 (1995).
77. Weckbecker, G. *et al.* Opportunities in somatostatin research: biological, chemical and therapeutic aspects. *Nat. Rev. Drug Discov.* **2**, 999–1017 (2003).
78. Katoh, T., Iwane, Y. & Suga, H. tRNA engineering for manipulating genetic code. *RNA Biol.* **15**, 453–460 (2017).
79. Cui, Z., Wu, Y., Mureev, S. & Alexandrov, K. Oligonucleotide-mediated tRNA sequestration enables one-pot sense codon reassignment in vitro. *Nucleic Acids Res.* **46**, 6387–6400 (2018).
80. Rutledge, S., Volkman, H. & Schepartz, A. Molecular recognition of protein surfaces:

- High affinity ligands for the CBPKIX domain. *J. Am. Chem. Soc.* **125**, 14336–14347 (2003).
81. Salveson, P. J. *et al.* Expansive discovery of chemically diverse structured macrocyclic oligoamides. *Science* **384**, 420–428 (2024).
  82. Vinogradov, A. A., Yin, Y. & Suga, H. Macrocyclic Peptides as Drug Candidates: Recent Progress and Remaining Challenges. *J. Am. Chem. Soc.* **141**, 4167–4181 (2019).
  83. Kawakami, T., Murakami, H. & Suga, H. Messenger RNA-Programmed Incorporation of Multiple N-Methyl-Amino Acids into Linear and Cyclic Peptides. *Chem. Biol.* **15**, 32–42 (2008).
  84. Katoh, T., Tajima, K. & Suga, H. Consecutive Elongation of D-Amino Acids in Translation. *Cell Chem. Biol.* **24**, 46–54 (2017).
  85. Diaz, D. B. *et al.* Illuminating the dark conformational space of macrocycles using dominant rotors. *Nat. Chem.* **13**, 218–225 (2021).
  86. Saunders, G. J. & Yudin, A. K. Property-Driven Development of Passively Permeable Macrocyclic Scaffolds Using Heterocycles\*\*. *Angew. Chem. Int. Ed.* **61**, e202206866 (2022).
  87. Hantzsch, A. Condensationsprodukte aus Aldehydammoniak und ketonartigen Verbindungen. *Berichte Dtsch. Chem. Ges.* **14**, 1637–1638 (1881).
  88. Knorr, L. Einwirkung von Acetessigester auf Phenylhydrazin. *Berichte Dtsch. Chem. Ges.* **16**, 2597–2599 (1883).
  89. Knorr, L. Synthese von Pyrrolderivaten. *Berichte Dtsch. Chem. Ges.* **17**, 1635–1642 (1884).
  90. Bose, D. S., Fatima, L. & Mereyala, H. B. Green Chemistry Approaches to the Synthesis of 5-Alkoxy-carbonyl-4-aryl-3,4-dihydropyrimidin-2(1H)-ones by a Three-Component Coupling of One-Pot Condensation Reaction: Comparison of Ethanol, Water, and Solvent-free Conditions. *J. Org. Chem.* **68**, 587–590 (2003).
  91. Kennedy-Smith, J. J., Staben, S. T. & Toste, F. D. Gold(I)-Catalyzed Conia-Ene Reaction of  $\beta$ -Ketoesters with Alkynes. *J. Am. Chem. Soc.* **126**, 4526–4527 (2004).

## Author Information

### Affiliations

Department of Chemistry, University of California, Berkeley, CA 94720.

Isaac Knudson, Hannah Cho, Cameron Paloutzian, Alanna Schepartz

Department of Molecular and Cellular Biology, University of California, Berkeley, CA 94720.

Alanna Schepartz

Department of Chemistry, Yale University, New Haven, CT 06520.

Taylor L. Dover, Diondra A. Dilworth, Scott Miller

California Institute for Quantitative Biosciences (QB3), University of California, Berkeley, CA 94720.

Alanna Schepartz

Chan Zuckerberg Biohub, San Francisco, CA 94158

Alanna Schepartz

Arc Institute, Palo Alto, CA

Alanna Schepartz

**Acknowledgments:** This work was supported by the NSF Center for Genetically Encoded Materials (C-GEM), CHE-2002182. T.L.D. and D.A.D. were supported by the NSF Graduate Research Fellowship Program under Grant Nos. DGE-2139841 and DGE-1122492. This research made use of the Pines Magnetic Resonance Center's Core NMR Facility (PMRC

Core), as well as the Chemical and Biophysical Instrumentation Center (CBIC) at Yale University (RRID:SCR\_021738), with equipment purchased with funds from NIH S10OD024998 (PMRC) or Yale University. We acknowledge Drs. Hasan Celik (PMRC Core), Raynald Giovine (PMRC Core) and Robert E. Berry (CBIC) for assistance with NMR data acquisition, Dr. Brandon Q. Mercado (CBIC) and Madison Houck (CBIC) for assistance with X-ray structural determination, and Dr. Fabian S. Menges (CBIC) for assistance with HRMS, MALDI-TOF, and IR data acquisition. We also acknowledge Melody C. Guo (Yale) for additional assistance with IR data acquisition, Andrew T. Champlin (Yale, Ellman Group) for assistance with chiral semi-preparative HPLC, S. Jafer Hasnain (Yale) for preliminary contributions, and members of the Schepartz and Miller groups for fruitful discussion.

**Author contributions:** I.J.K., D.A.D., A.S., and S.J.M. designed the project. I.J.K. led acylation experiments, Friedländer reaction optimization, *in vitro* translation, solid phase peptide synthesis and post-translational reactions. I.J.K., T.L.D., and D.A.D. synthesized materials and analyzed/interpreted results. H.C. and C.P. assisted with acylation experiments. I.J.K., T.L.D., A.S., and S.J.M. prepared the manuscript.

### **Ethics Declarations**

Competing interests: I.J.K., S.J.M, and A.S. have submitted a patent application related to this work.